Bull Volcanol (2001) 63:179–190
DOI 10.1007/s004450100134

RESEARCH ARTICLE

Hugh Tuffen · Jennie Gilbert · Dave McGarvie

Products of an effusive subglacial rhyolite eruption: Bláhnúkur, Torfajökull, Iceland

Received: 24 February 2000 / Accepted: 8 February 2001 / Published online: 9 May 2001

Abstract We present field observations from Bláhnúkur, a small volume (<0.1 km^3) subglacial rhyolite edifice at the Torfajökull central volcano, south-central Iceland. Bláhnúkur was probably emplaced during the last glacial period (ca. 115–11 ka). The characteristics of the deposits suggest that they were formed by an effusive eruption in an exclusively subglacial environment, beneath a glacier >400 m thick. Lithofacies associations attest to complex patterns of volcano-ice interaction. Erosive channels at the base of the subglacial sequence are filled by both eruption-derived material and subglacial till, which show evidence for deposition by flowing meltwater. This suggests that meltwater was able to drain away from the vent area during the eruption. Much of the subglacial volcanic deposits consist of conical-to-irregularly shaped lava lobes typically 5–10 m long, set in poorly sorted breccias with an ash-grade matrix. A gradational lava-breccia contact at the base of lava lobes represents a fossilised fragmentation interface, driven by magma–water interaction as the lava flowed over poorly consolidated, waterlogged debris. Sets of columnar joints on the upper surfaces of lobes are interpreted as ice-contact features. The morphology of the lobes suggests that they chilled within conically shaped subglacial cavities 2–5 m high. Avalanche deposits mantling the flanks of Bláhnúkur appear to have been generated by the collapse of lava lobes and surrounding breccia. A variety of deposit characteristics suggests that this occurred both prior to and after quenching of the lava lobes. Collapse events may have occurred when the supporting ice walls were melted back from around the cooling lava lobes and breccias. Much larger lava flows were emplaced in the latter stages of the eruption. Columnar joint patterns suggest that these flowed and chilled within subglacial cavities 20 m high and 100–200 m in length. There is little evidence for magma–water interaction at lava flow margins which suggests that these larger cavities were drained of meltwater. As rhyolite magma rose to the base of the glacier, the nature of the subglacial cavity system played an important role in governing the style of eruption and the volcanic facies generated. We present evidence that the cavity system evolved during the eruption, reflecting variations in both melting rate and edifice growth that are best explained by a fluctuating eruption rate.

Keywords Subglacial · Rhyolite · Magma–ice interaction · Columnar jointing · Obsidian · Phreatomagmatic

Editorial responsibility: W. Hildreth

H. Tuffen (✉) · D. McGarvie
Department of Earth Sciences, The Open University, Milton Keynes, MK7 6AA, UK
e-mail: h.tuffen@lancaster.ac.uk
Tel.: +44-1524-65201 ext. 93574, Fax: +44-1524-593985

H. Tuffen · J. Gilbert
Department of Environmental Science, Lancaster University, Lancaster LA1 4YQ, UK

Introduction

Subglacial rhyolite has been described at the Icelandic central volcanoes of Kerlingarfjöll (Grönvold 1972) and Torfajökull (Sæmundsson 1972, 1988). It occurs at other central volcanoes (e.g. Katla, Hofsjökull) and in isolated volcanoes (e.g. Hágöngur). The only published account of facies and emplacement mechanisms of subglacial rhyolite (Furnes et al. 1980) included generalised descriptions of lava lobe-hyaloclastite formations at Bláhnúkur and elsewhere. Two discrete types of hyaloclastite were identified, one dominated by pumice clasts (type 1) and a mixed obsidian–microcrystalline rhyolite lava hyaloclastite (type 2). Type 1 was envisaged to have formed during explosive magma degassing from lobes of rhyolite lava, and type 2 from brittle spalling of lobe fragments.

Various authors have conducted detailed lithofacies analysis of subaqueously emplaced rhyolite (Yamagishi and Dimroth 1985; Cas et al. 1990; Hanson 1991; Scutter et al. 1998; Hunns and McPhie 1999) and subglacial basalt (Smellie et al. 1993; Skilling 1994; Smellie and Skilling 1994; Smellie and Hole 1997; Werner et al. 1996; Werner and Schmincke 1999). These studies have shed light on mechanisms of rhyolite lava–water interac-

Table 1 Major differences between subaqueous and subglacial eruptions

Property of eruption	Subglacial environment	Subaqueous environment	Implications
Edifice constraint	Constraint by ice walls during subglacial stage[a]	No constraint	Subglacial edifices likely to be steeper with greater risk of flank collapse if ice recedes
Effective pressure	Varies from glaciostatic to atmospheric, depending on meltwater discharge rate[b]	Variable but hydrostatic	Style of subglacial eruptions likely to be more variable: effusive and explosive
Water/magma ratio	Variable depending on drainage patterns	Consistently high, although steam envelopes may "shield" magma[c]	Subglacial sequences may include "dry" units with little evidence for magma–water interaction

[a] Skilling (1994); [b] Hooke (1984); [c] Kokelaar (1982)

Table 2 Major differences between subglacial rhyolite and basalt eruptions

Property of eruption	Subglacial rhyolite	Subglacial basalt	Implications
Magma temperature[a]	800–900°C	1100–1200°C	Less energy released as rhyolite is quenched
Melting potential[a]	≤8 times own volume of ice	≤14 times own volume of ice	Positive pressure changes during rhyolite eruption, negative during basalt
Pressure changes during eruption[a]	Positive	Negative	Rhyolite: meltwater tends to drain away; basalt: meltwater tends to collect at vent
Magma viscosity[a]	10^6–10^7 Pa s	10^3–10^4 Pa s	Rhyolite eruptions tend to be more explosive, larger aspect ratio lava flows
Effusion rate[a]	10^1–10^2 $m^3 s^{-1}$	10^1–10^4 $m^3 s^{-1}$	Inward ice creep[b] more significant during rhyolite eruptions because edifice growth is slower[a]
Distribution[c]	Iceland, mostly at central volcanoes	Antarctica, Iceland, British Columbia	Basalt much better studied than rhyolite
Recent eruptions	None observed	Gjálp 1996, Iceland[c]	Insight gained on basaltic eruptions, not on rhyolitic

[a] Hoskuldsson and Sparks (1997); [b] Guðmundsson et al. (1997); [c] Smellie (1999)

tion (e.g. Yamagishi and Dimroth 1985; Hunns and McPhie 1999) and on the interplay between eruptive mechanisms and glacier response (e.g. Smellie and Skilling 1994). Eruptions of rhyolite and basalt magmas under ice are likely to differ from eruptions under water because of significant differences in the physical environment (Table 1). Different magma types are also likely to produce different subglacial eruption styles (Table 2). Silicic tephra layers in Greenland ice cores are thought to originate from subglacial rhyolite eruptions in Iceland (Zielinski et al. 1997). A similar origin has been attributed to tephra layers in Icelandic glaciers (Larsen et al. 1998), on the Atlantic sea floor (Lacasse et al. 1995) and in Scottish peat (Dugmore et al. 1995). Ice-covered rhyolite volcanoes thus appear capable of major explosive eruptions, emphasising the need for further study.

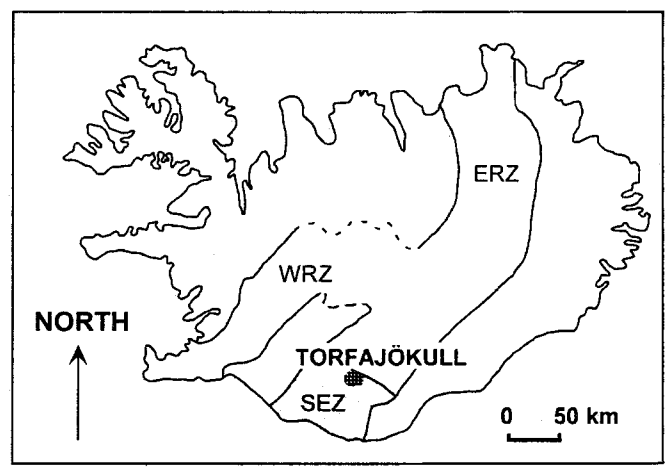

Fig. 1 Map of Iceland showing the location of Torfajökull central volcano. *ERZ* Eastern Rift Zone; *WRZ* Western Rift Zone; *SEZ* South Eastern Zone

Geological setting

The Torfajökull volcanic complex, Iceland's largest rhyolite centre, is located where the southerly propagat-

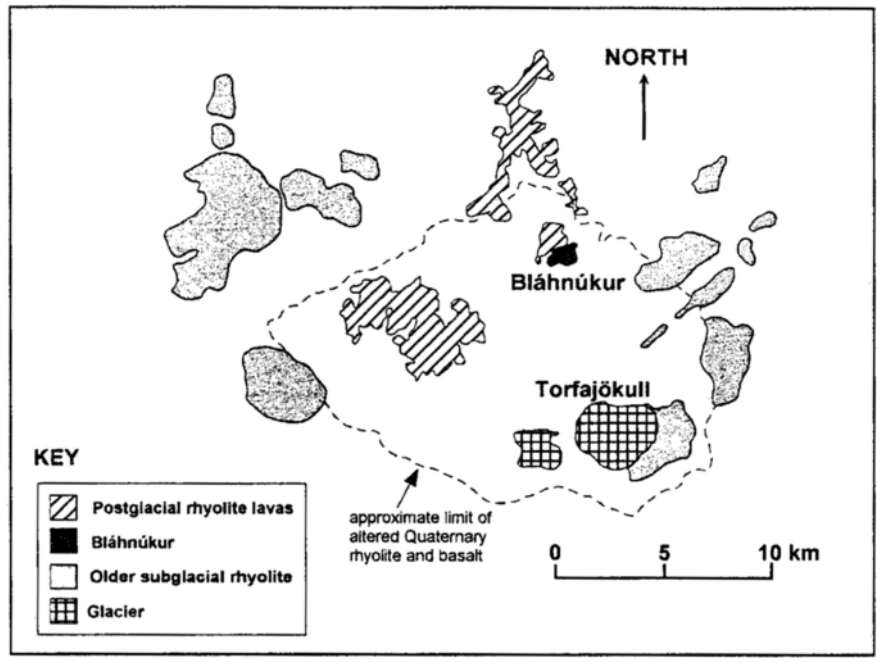

Fig. 2 Simplified geological map of the Torfajökull volcanic complex. The *dotted line* indicates the approximate extent of Quaternary altered rhyolite and basalt. The rest of the *white area* is composed of basaltic formations of Vatnafjöll and Veiðivotn

ing Eastern Rift Zone meets the South Eastern Zone, an older crustal segment (Fig. 1). Activity began in mid-Quaternary time (Sæmundsson 1972), forming a now highly dissected rhyolite plateau measuring 18×12 km. The total volume of this plateau, 250 km^3, is dominated by rhyolite erupted in subglacial and subaerial environments, with minor basaltic hyaloclastites and fluvioglacial sediments. The youngest subglacial rhyolite volcano at Torfajökull appears to be Bláhnúkur. This is an isolated, small-volume edifice in the northern part of the complex (Fig. 2).

Overall structure of Bláhnúkur

Bláhnúkur rises 350 m above a dissected plain of altered Quaternary rhyolite. Roughly pyramidal in form, it has a core of older rhyolite draped by a veneer of young subglacial rhyolite, henceforth called Bláhnúkur rhyolite (Fig. 3). The drape adds approximately 50 m to its height (Fig. 3). Massive orange-brown diamicton underlies the subglacial sequence on the south flanks of Bláhnúkur. This diamicton, which locally exceeds 20 m in thickness, contains cobbles of altered basalt and rhyolite lava set in a muddy matrix. The Bláhnúkur rhyolite appears to have been emplaced along four distinct fissures, trending from WSW–ENE to NW–SE (Fig. 4). These fissures do not follow the regional tectonic fabric (NE–SW). Bláhnúkur rhyolite, which differs from the subglacial rhyolite of neighbouring volcanoes in both its freshness and chemistry (Sæmundsson 1972; Ivarsson 1992), appears to be the product of an isolated, small-volume effusive eruption during the last glacial period (i.e. 115–11 ka ago). Bláhnúkur rhyolite contains a minor proportion of basaltic inclusions, a feature also typical of postglacial rhyolite lava flows at Torfajökull (McGarvie 1984).

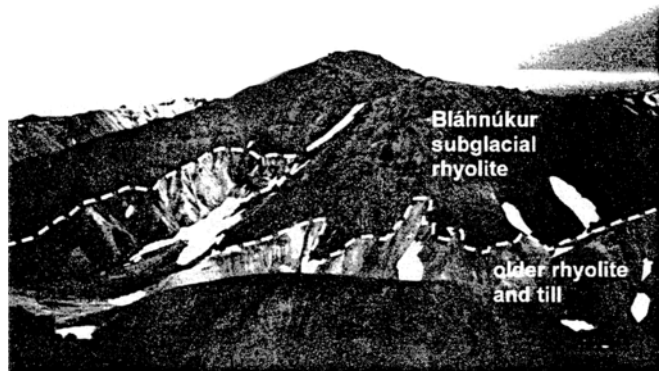

Fig. 3 View of Bláhnúkur from the west. A veneer of young subglacial rhyolite overlies older rhyolite and till. Vertical distance from base to summit is 350 m

Evidence for a subglacial environment

Although there is no single feature that provides unambiguous evidence for a subglacial eruptive setting, the following features suggest that Bláhnúkur rhyolite was erupted under ice:

1. Much of the sequence consists of breccias, which show evidence for magma–water interaction (perlitised obsidian, blocky ash shards, fines-rich veins, matrix vesicles). There is no evidence for the existence

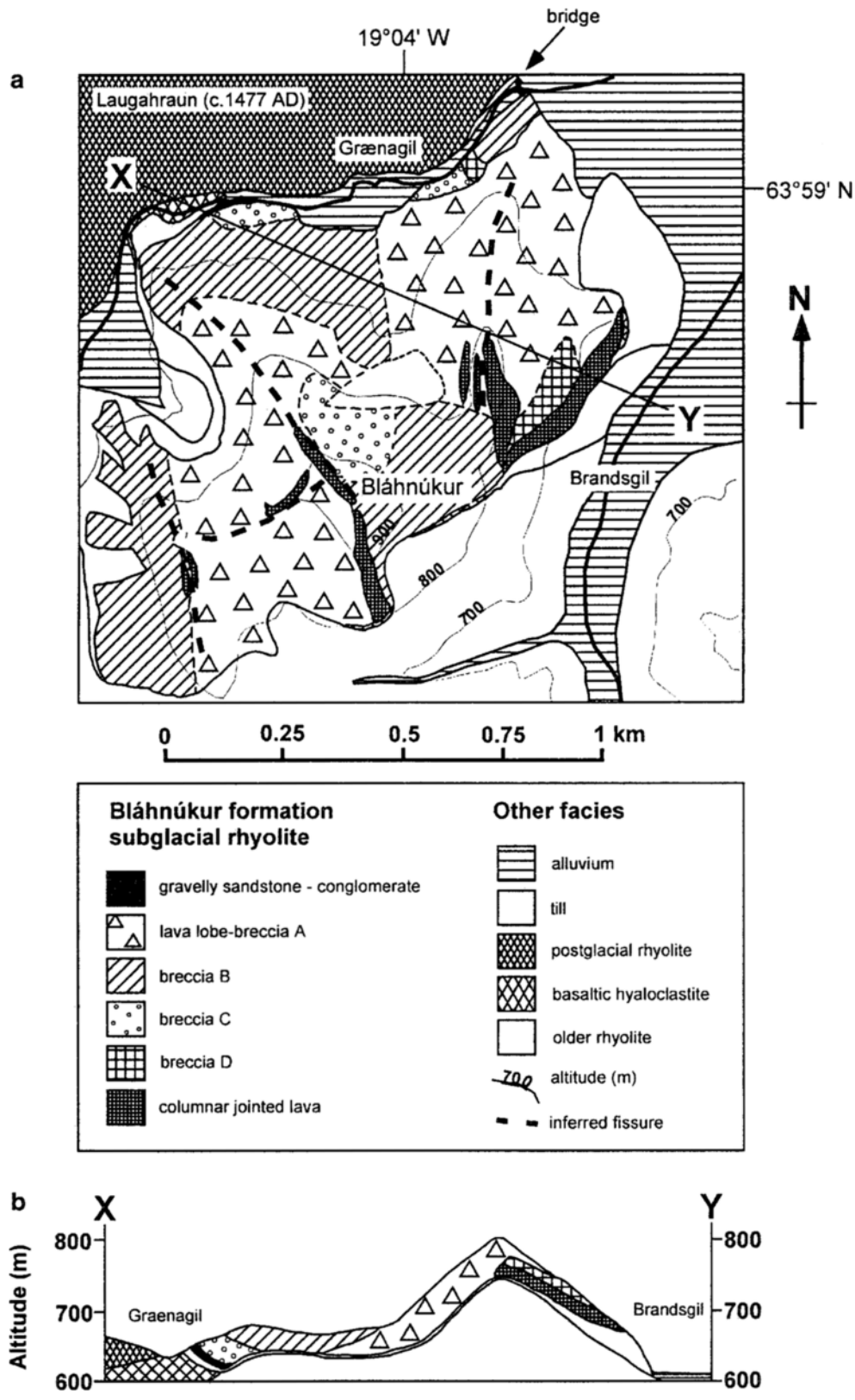

Fig. 4 **a** Simplified geological map of Bláhnúkur, which is bounded to the north and east by the streams Grænagil and Brandsgil, respectively. The postglacial rhyolite lava flow Laugahraun occurs on the north side of Grænagil. **b** Simplified cross section

of a palaeotopography which could have confined a non-glacial lake (c.f. Jones 1968; Smellie and Skilling 1994; Smellie and Hole 1997). The lack of fossils, as well as the current elevation of 600–945 m in the absence of any tectonic structures consistent with uplift, precludes a submarine setting. Glacier melting is thus the most likely source of water.

2. Columnar jointing patterns suggest that many lava bodies in the sequence chilled against steeply inclined, sub-planar surfaces. Such jointing patterns, which have not been found in subaqueous or subaerial rhyolite lavas (e.g. Scutter et al. 1998; Fink 1983) are best explained by the chilling of lavas against ice walls (Lescinsky and Sisson 1998).
3. One lithology within the Bláhnúkur complex contains rounded, facetted clasts and a mud matrix consistent with a subglacial derivation (i.e. till).

Lithofacies descriptions and interpretations

Volcaniclastic lithofacies were distinguished in the field using bedding characteristics, plus the type, size and morphology of clasts (McPhie et al. 1993). The crystallinity, morphology, vesicularity and jointing patterns of coherent volcanic lithofacies are also described. "Juvenile" is used to refer to products of the subglacial Bláhnúkur rhyolite eruption, whereas "lithic" refers to clasts derived from the underlying basement.

Mixed juvenile-lithic lithofacies

Gravelly sandstone and conglomerate

Description. The gravelly sandstone and conglomerate lithofacies occurs as a 5–14 m thick sequence on the southern bank of Grænagil 1 km WSW of the bridge (Fig. 5). At the base, a 0.5- to 5-m-thick unit of orange-brown massive to planar bedded matrix-supported lithic conglomerate lies in an inclined erosive channel cut into basaltic pillow breccia. Upper and lower surfaces are sharp, the channel pinching out laterally over ~100 m. The conglomerate contains sub-rounded to rounded, facetted cobbles of altered aphyric rhyolitic and basaltic lava up to 30 cm in diameter in a mud-grade orange-brown matrix. It is devoid of juvenile material.

A 1- to 6-m-thick gravelly sandstone unit overlying the conglomerate (Fig. 5) is moderately well sorted and laterally continuous over at least 100 m. In general, the gravelly sandstone comprises sub-planar beds 10–30 cm thick. However dune-like cross-stratification is also developed, with a wavelength of ~3 m. Over 95% of clasts consist of juvenile phenocryst-rich black obsidian and grey perlitised vesicular obsidian. Clasts are angular to sub-angular and 0.5–2 cm across. Sub-rounded 0.5- to 1-cm lithic clasts of altered aphyric rhyolite and basalt lava make up the remainder of the deposit. The matrix consists of sand-grade angular clasts of juvenile obsidian.

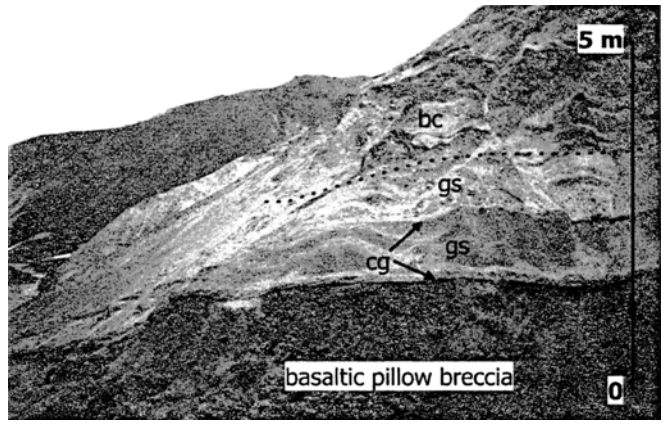

Fig. 5 A 10-m-high outcrop on the south bank of the stream Grænagil, 1 km WSW of the bridge. Gravelly sandstone and conglomerate unconformably overlie basaltic pillow breccia. The gravelly sandstone is overlain by breccia C (upper 6 m of section). *cg* Conglomerate; *gs* gravelly sandstone; *bc* breccia C

A 3-m-thick brown breccia-conglomerate unit is locally present at the top of the sequence, comprising 10- to 20-cm-thick matrix-supported lithic-rich breccia horizons intercalated with 3- to 10-cm-thick beds of conglomerate. This unit is overlain by 1 m of cemented brown conglomerate. At the northern limit of this exposure, lithics in the gravelly sandstone disappear 3 m above the erosive base (Fig. 5). It is overlain by poorly sorted juvenile breccias (breccia C).

Interpretation. The channelised, poorly sorted conglomerate is similar to units on Mt. Pinafore, Alexander Island, Antarctica (Smellie et al. 1993; Smellie and Skilling 1994), which were interpreted as meltout tills formed by the redeposition of till by meltwater within a subglacial cavity. A similar interpretation is made here. The sorting, horizontal and cross-stratification and sharp boundaries of the gravelly sandstone units suggest deposition from a traction current (Smellie et al. 1993). The presence of interbedded lithic- and juvenile-dominated units suggests that pulses of juvenile material entered the subglacial cavity, probably washed from the vent area by a stream of volcanically generated meltwater. This syn-eruptive lithofacies occurs 350 m vertically below the highest subglacial rhyolite deposits; hence, we infer that meltwater drainage occurred during the eruption beneath a glacier at least 350 m thick.

Juvenile lithofacies

Lava lobe-breccia A

Description. Lava lobe-breccia A lithofacies dominates the western flank of Bláhnúkur (Figs. 4, 6a). It is best exposed approximately 250 m northwest of the summit and on the south bank of Grænagil between 100 and 150 m upstream of the bridge. It consists of 5- to 20-m

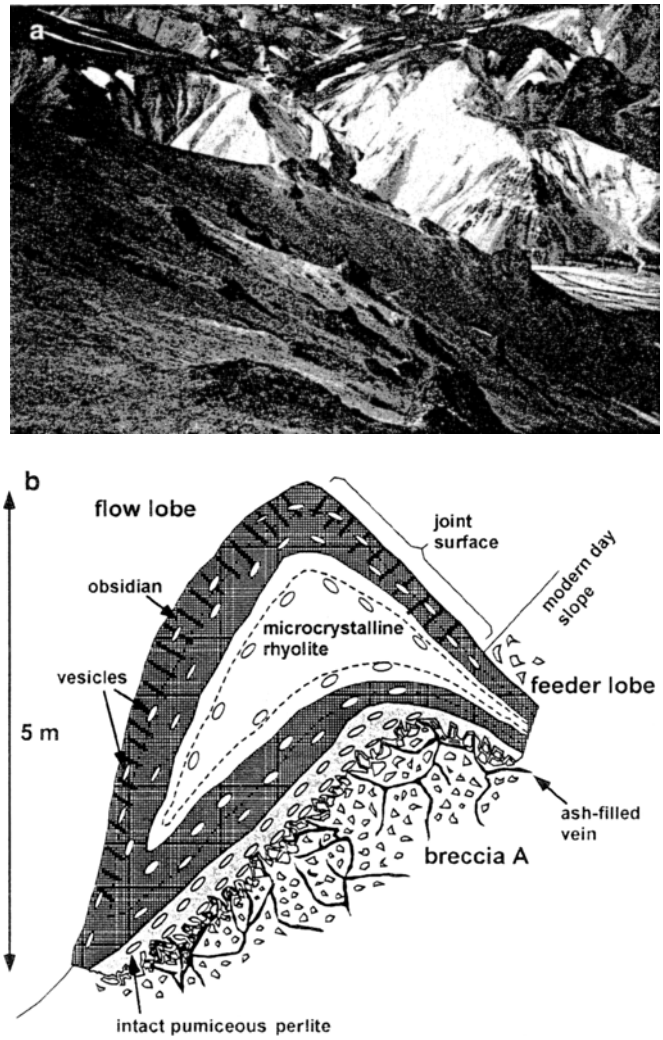

Fig. 6 **a** Looking southwest from 250 m northwest of Bláhnúkur summit. The west flank of Bláhnúkur (foreground) shows numerous 5- to 10-m lava lobes (*dark outcrops*) set in pumiceous breccia (*pale grey*, mostly concealed by scree). The *white material* in the background is older rhyolite, which has been draped by the postglacial lava flow Laugahraun (*dark material in top right corner*). **b** The overall structure of an idealised lava lobe

dark, irregularly to cylindrically shaped obsidian and microcrystalline rhyolite lobes set in pale grey breccia. Lobes can be subdivided into flow lobes and feeder lobes. Flow lobes have curvicolumnar jointed obsidian upper surfaces, whereas their bases are gradational with the surrounding breccia (Fig. 6b). Flow banding is roughly parallel to the present-day slope. Vesicularity increases from <5% within the microcrystalline rhyolite core to ~10% in the 5- to 50-cm-thick upper obsidian selvage. At the base of flow lobes, the obsidian becomes paler and increasingly perlitised. The proportion of elongate vesicles increases to 20–30% at the base, giving the obsidian a pumiceous appearance. The perlitised material becomes increasingly fractured at the outer margin, and grades outwards into massive, poorly sorted breccia, containing angular clasts of pale-grey perlitised obsidian in an ash matrix (Fig. 6b). This matrix contains spherical vesicles generally 1–3 mm but up to 20 mm long. Perlitised obsidian clasts are 0.5–30 cm across and contain 15–40% elongate vesicles. Ash particles are glassy with blocky morphologies and typically 10–100 μm across. The breccia is cut by anastamosing irregular veins 5–30 mm wide, filled with vesiculated ash. These terminate at the obsidian lobe margin (Fig. 6b).

Feeder lobes are irregular to sheet-like in morphology and typically 5–20 m across. They are distinguished from flow lobes by the orientation of their flow banding, which dips into the edifice, mostly at 30–60°. An obsidian margin 10–50 cm wide envelops a hackly jointed microcrystalline interior, which is often orange coloured due to alteration. Locally, flow banding in feeder lobes is seen to continue into a flow lobe (Fig. 6b).

Interpretation. The gradational contact between the base of flow lobes and breccia suggests in situ fragmentation of the lobes. Pumiceous, perlitised clasts and ash were created at lobe bases, which were in contact with earlier-formed breccia. A similar suite of textures occurs in rhyolitic pumiceous peperite emplaced in a submarine setting at Mt. Chalmers Queensland, Australia (Hunns and McPhie 1999). The increase in vesicularity from the core to rim of lobes (Furnes et al. 1980) suggests that magmatic volatiles diffused outward from the lobe interior. Moderate vesicularity results from emplacement at a relatively low confining pressure (likely glaciostatic pressure <4 MPa) and the formation of a glassy rind, which favoured volatile retention (Hunns and McPhie 1999). The presence of microcrystalline lava lobe cores indicates that the cooling time of individual lobes was sufficiently long for crystallisation. However, cooling timescales can only be estimated (e.g. Hoskuldsson and Sparks 1997), since the rate of microlite growth in rhyolitic magma is poorly constrained (e.g. Higgins 1996). Furnes et al. (1980) labelled this lithofacies type-1 hyaloclastite, and suggested that fragmentation was driven by magma vesiculation. We question this interpretation, since the blocky morphology of ash shards suggests that fragmentation was dominantly phreatomagmatic and driven by quenching, rapid glass contraction and steam explosivity (Heiken and Wohletz 1985). We suggest that the lava lobes represent the subglacial equivalent of an effusive rhyolite eruption, in which fragmentation due to volatile exsolution was minimal. Furthermore, perlitic alteration is an indication that water interacted with lobe margins, and vesiculated ash may indicate that a vapour phase was present (Lorenz 1974; Hunns and McPhie 1999). By contrast, the top and sides of lobes are glassy and intact, with columnar joints normal to steeply inclined, subplanar surfaces (Fig. 6b). Similar columnar joint patterns in lavas on Mt. Rainier, Washington, are thought to be an ice-contact feature, formed as lava chilled against steeply inclined ice walls (Lescinsky and Sisson 1998). We adopt a similar interpretation here, and infer that lobe sides chilled against ice with explosive magma–meltwater interaction.

The orientation of lobes is bimodal, with feeder lobes dipping into the modern slope and flow lobes dipping at an angle parallel to the modern slope. A similar bimodal pattern was seen in subaqueous rhyolite hyaloclastite in Japan (Yamagishi and Dimroth 1985). The interpretation at Bláhnúkur is that magma rose in sheets or fingers to the base of the glacier, where it flowed a limited distance down-slope over water-saturated breccias, before freezing against a constraining ice wall (Furnes et al. 1980). Rising magma locally ponded within the breccia, forming irregular intrusions.

Breccia B

Description. Breccia B lithofacies is best seen on the south bank of Grænagil, in cliffs 10–30 m high directly south–southwest of the bridge (Fig. 4). Much larger but less well-exposed outcrops are found on the north flank of the central ridge, the west flank of the west ridge and directly east of the summit. In Grænagil, massive to crudely bedded matrix- and clast-supported green breccias host elongate to lenticular ribbons and blobs of obsidian (Fig. 7a). Ribbons are typically 0.5–5 m long and 5–50 cm wide. The breccias consist of pumiceous, perlitised obsidian clasts, typically 0.5–5 cm across, set in an ash matrix of angular glass shards. The ash contains spherical to irregular voids 1–3 mm in diameter. Irregular, anastamosing pale green ash-filled veins 0.5–3 cm wide cut the outcrop. Obsidian ribbons are displaced up to 15 cm where they are cut by these veins. Vesicles in the ribbons are locally sheared parallel to veins (Fig. 7b), indicating ductile deformation. The abundance of vesicles is fairly uniform within the ribbons, and does not increase close to the sharp contact with the surrounding breccia. A centimetre-wide zone of brown, indurated ash occurs at the margin of some ribbons. Many ribbons are aligned along a plane that dips at approximately 10° into the modern-day slope (Fig. 7a). The deposit is cut by numerous low-angle near-planar faults, on which the sense of displacement is unclear.

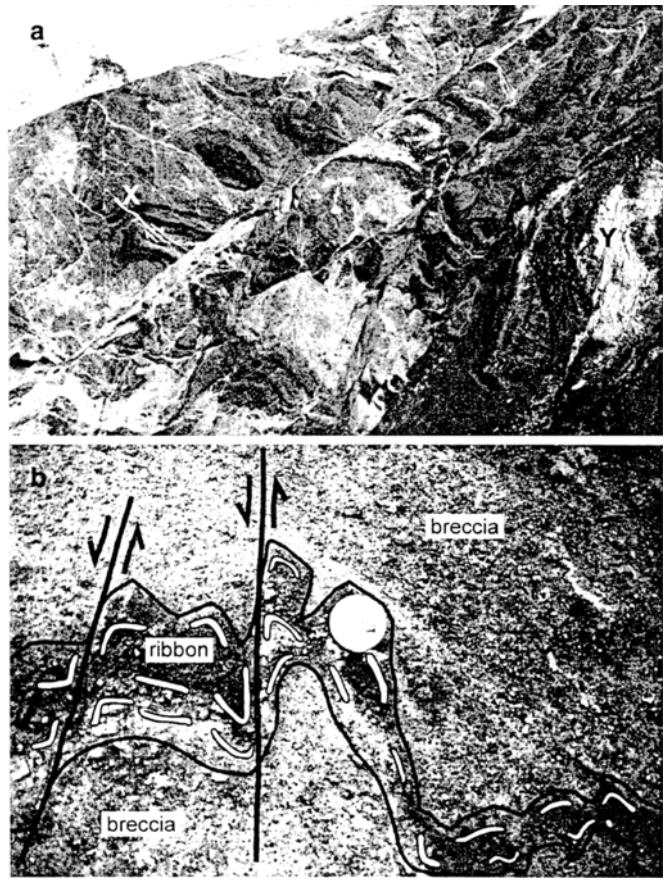

Fig. 7 **a** A 20-m-thick exposure of breccia B 50 m WSW from the bridge across Grænagil. Massive pumiceous breccia (*medium-grey*) hosts obsidian ribbons (*dark bodies*). Pale veins are filled with vesiculated ash; these cut and displace obsidian ribbons (*X*). The pale body at *Y* is the microcrystalline core of a lava lobe. **b** Close-up of an obsidian ribbon offset by small thrust faults (*thick black lines*) within breccia B. The *white deformed ellipses* indicate the approximate orientation of vesicles in the obsidian and are not to scale. Vesicles have been bent along fault planes, indicating ductile deformation. Pale domains of the ribbon are perlitised, and weathering has given the intact obsidian of the ribbon a brecciated appearance. *Lens cap* is 50 mm in diameter

Interpretation. Deformed vesicles adjacent to veins cutting some obsidian ribbons (Fig. 7b) indicate that the ribbons were deformed while still hot (White and Busby-Spera 1987; Hunns and McPhie 1999). However, the sharp contact between the ribbons and surrounding breccia indicates that the lobes did not generate the surrounding breccia. Instead, hot ribbons and blobs and the enclosing breccia appear to have been deposited together in a hot debris avalanche. This is likely to have been due to the syn-emplacement gravitational collapse of lava lobe-breccia A. Collapse events may have been triggered as the supporting ice melted back. Fines in the breccia may have been remobilised by steam fluxing shortly after emplacement. Instability at this stage could have created numerous semi-brittle fault planes, into which ash was transported, generating ash-filled veins. Vesiculated ash may be further evidence for an active vapour phase (Lorenz 1974; Hunns and McPhie 1999). It is notable that the glass of the obsidian ribbons is microlite-poor, in contrast with the microlite-rich cores of lava lobes. This is consistent with the model that lava lobes fell apart while still above the glass transition temperature, leading to relatively rapid cooling. This lithofacies is interpreted as a hot avalanche deposit and illustrates the instability of the subglacial rhyolite edifice during its growth.

Breccia C

Description. Breccia C lithofacies crops out in Grænagil (500–1000 m WSW of the bridge) and on the north flank, 50 m north of the summit (Fig. 4). In Grænagil it forms a chaotic sequence 10- to 20-m-thick, comprising fragments of rhyolite lava lobes 1–20 m long in contact

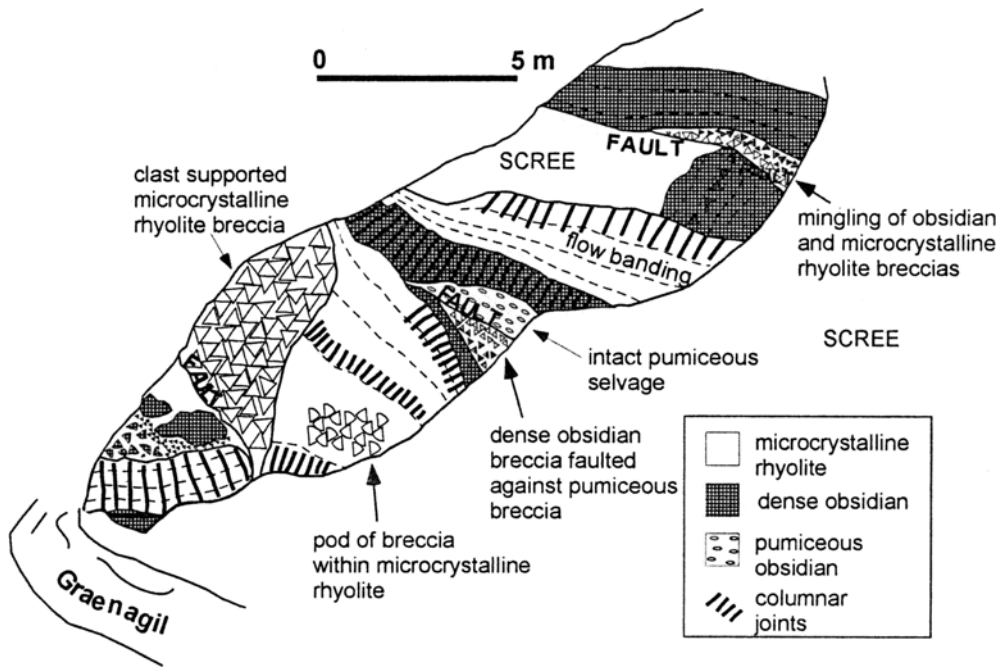

Fig. 8 Field sketch of breccia C in Grænagil 600 m WSW of the bridge. A stack of subparallel lobe portions 1–20 m long is cut by numerous faults, juxtaposing obsidian, microcrystalline rhyolite and pumiceous breccia

with lenses of breccia and cut by abundant small faults (Fig. 8). Lenses of massive, moderately well-sorted pumiceous and dense obsidian breccia (0.2–1 m across) are faulted against lobe portions, which consist of hackly to columnar jointed flow-banded microcrystalline rhyolite and obsidian. Pods of rubbly breccia locally cut the microcrystalline rhyolite, discordant to flow banding. There is a 5-cm-thick zone of clast-supported breccia at the faulted contact between obsidian and microcrystalline lobe portions. The breccia consists of obsidian clasts adjacent to the intact obsidian domains of lava lobes and microcrystalline rhyolite clasts adjacent to the microcrystalline rhyolite domains, with a zone of clast mingling ~1 cm wide on the fault plane (Fig. 8). A major set of sub-parallel faults dips into the slope at 60–70°. These cut a second set of randomly orientated, smaller faults. Clasts in the microcrystalline rhyolite and obsidian breccias are vesicle-poor (<1% irregular vesicles <4 mm long) and blocky in shape, typically 5–20 cm across. By contrast, 0.5- to 5-cm angular clasts in the pumiceous breccia contain 20% elongate vesicles. On the north flank, this lithofacies forms a downslope-dipping veneer <5 m thick, overlying lava lobe-breccia A. Veins of fine-grained ash in lava lobe-breccia A lithofacies abruptly terminate at the base of breccia C.

Interpretation. Breccia C consists largely of fragments of lava lobes with lesser amounts of pumiceous breccia. The faulted juxtaposition of several diverse lithologies, with brecciation and clast mingling at faulted contacts indicates lateral movement, possibly during sliding of lava lobe-breccia A down the flanks of the accumulating pile. Our interpretation is that accompanying fragmentation has been slight, resulting in the stacking of numerous near-intact lobe fragments against each other. There is no evidence for high temperatures or the presence of water during emplacement. This lithofacies is thus thought to record en masse slumping events, in which quenched lobes and breccia slid downslope.

Breccia D

Description. Breccia D lithofacies crops out on the south bank of Grænagil approximately 150 m upstream of the bridge and on the eastern flank, where it forms a prominent outcrop ~20 m high; Fig. 4). It is a poorly sorted matrix-supported polymict breccia, containing 1–30 cm angular clasts of microcrystalline rhyolite, dense black obsidian and grey-white pumiceous, perlitised obsidian set in an ash matrix. Faint bedding, which is picked out by trails of large clasts, dips at approximately 10° into the local slope. Angular clasts of microcrystalline rhyolite are bounded by joint planes, which truncate flow banding. Pumiceous clasts contain ~30% vesicles by volume, and ash particles resemble those found in breccia A. Irregular bodies of perlitised obsidian intrude the deposit on the east flank. These display tiny (1–2 cm wide) columns close to the contact with the breccia.

Interpretation. This facies corresponds to the type-2 hyaloclastite of Furnes et al. (1980) who suggested that it was formed by explosive fracture of the chilled carapace of lava lobes. Whereas such a mechanism may have generated obsidian and rhyolite clasts, we suspect that breccia D represents remobilized lava lobe-breccia A. Poor sorting is consistent with emplacement in a cohesive mass flow (Smellie and Skilling 1994). Clasts are entirely juvenile and exactly match the range of textures observed in lava lobe-breccia A. Joint-bounded microcrys-

talline rhyolite clasts indicate that the core of lobes had substantially cooled prior to fragmentation. From our observations of breccia B we know that lava lobe-breccia A was unstable during emplacement. Our preferred model for the emplacement of breccia D involves the gravitational collapse of quenched lava lobes and breccia, caused by the withdrawal of supporting ice walls. Accompanying fragmentation appears to have been more extensive than in breccia C, since no lobe portions have survived intact. This may indicate a greater transport distance or a more energetic debris flow than that which generated breccia C.

Columnar-jointed lava

Description. Large columnar-jointed lava flows occur on the eastern and southern flanks of Bláhnúkur. A lava flow 200 m long and 20-m-thick drapes the steep southern flank directly south of the summit (Fig. 4). It has a triangular cross section and is bounded by three sub-planar columnar jointed surfaces: two steeply inclined walls (~60–70° dip) and a base parallel to the modern day slope (~30° dip). Columnar joints are 10–30 cm apart and normal to flow margins. They penetrate to the centre of the flow. An obsidian selvage up to 5 m thick envelops a microcrystalline rhyolite interior, which contains <1% irregular vesicles. At the southern tip of the lava, the base grades into hydrothermally altered, perlitised obsidian breccia.

The largest lava flow observed is on the east flank (Fig. 4). It is sheet-like in morphology, ~20 m thick and 400 m wide. The main lava body appears to feed numerous tube-like apophyses, such as the 20-m-thick lava pictured in Fig. 9a. The tube-like lava is triangular in cross section, with a set of columnar joints normal to both the steeply inclined sides and the gently inclined base. Flow banding is parallel to the lava margins. There is a sharp contact between the microcrystalline flow interior and 4-m-thick intact obsidian selvages (Fig. 9a). Perlite and breccia are absent from the lava base, and there is a locally peperitic contact with the underlying poorly consolidated till. At the southwestern limit of the sheet-like lava, columnar joints describe a spectacular box-like form (Fig. 9b). Columnar joints in the glassy lava top, sides and base are spaced 10–15 cm apart and are normal to flow margins.

Interpretation. Andesite lava flows on Mt. Rainier, Washington, have similar attributes: steeply inclined flow sides with subhorizontal columns and thick glassy margins (Lescinsky and Sisson 1998). Columnar joints develop normal to cooling surfaces (DeGraff et al. 1989), so the orientation of columns can be used to reconstruct three-dimensional cooling patterns. Hence, the columnar-jointed sides of the Mt. Rainier lavas were interpreted as ice-contact features, formed as the lava flowed and chilled against ice walls. Unlike those on Mt. Rainier, the lavas of Bláhnúkur also have columnar-jointed flow tops, which suggest cooling either by meltwater running over the lava (Sæmundsson 1970) or by direct contact with a subhorizontal ice roof. We thus infer a subglacial setting for the columnar jointed lavas, which may have flowed and chilled within tunnel-like cavities melted into the basal ice. There is limited evidence for magma–water interaction, with perlitisation and peperite restricted to lava bases, suggesting that there was little meltwater present within the cavities during emplacement of the lavas.

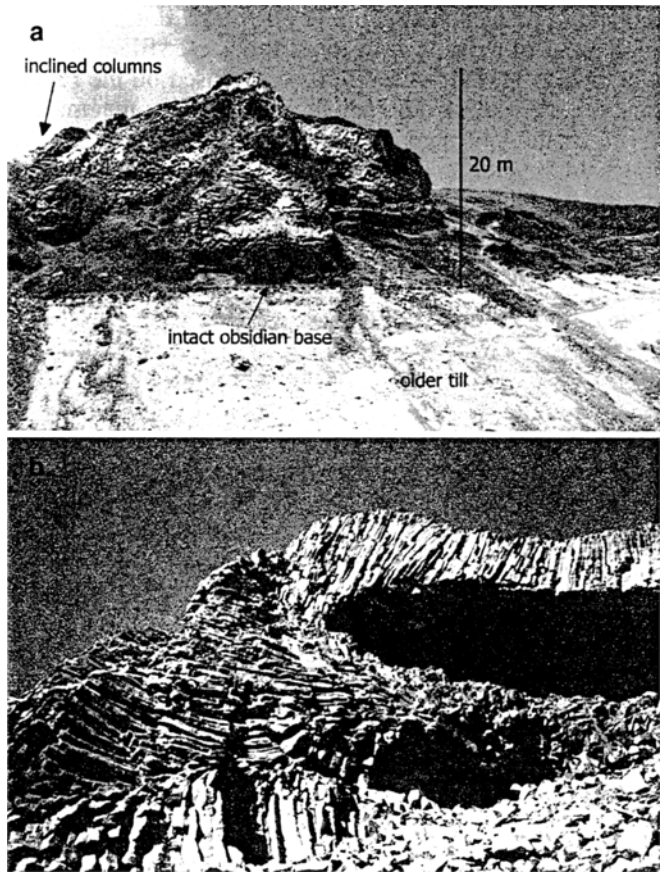

Fig. 9 **a** A 20-m-thick columnar-jointed lava flow directly overlying till on the eastern flank of Bláhnúkur, above Brandsgil (800 m due south of the bridge). There is a 4-m-thick selvage of intact obsidian at its base. Slender columns are inclined or subhorizontal. The surface currently exposed is a cross section of the lava flow, which flowed down a ~20° incline towards the camera. **b** A 20-m-thick columnar-jointed rhyolite lava flow on the eastern flank. Joint patterns suggest that the lava chilled against a subhorizontal ice roof (*top*) and steeply inclined ice walls (*left*)

Discussion

Relative rates of ice melting and lava flow

We compare ice melting rates to the advance rate of a rhyolite lava body, to determine whether rhyolite lava melts its way through the ice, or flows within pre-existing cavities. Hoskuldsson and Sparks (1997) estimated that

ice would be melted at a rate of 10^{-6} m s^{-1} during the emplacement of rhyolite lava lobes in a water-filled subglacial cavity. This slow melting rate is based on the rate of heat transfer during conductive cooling of the magma and the formation of a chilled rind (Allen 1980). Although much higher melting rates of 10^{-3} m s^{-1} were observed during the Gjálp subglacial basalt eruption, this is thought to indicate more rapid heat exchange caused by explosive magma–water interaction (Guðmundsson et al. 1997).

The effective viscosity of a 100-m-thick rhyolite lava flow with a chilled carapace is likely to exceed the magma viscosity by 1.8–3.6 orders of magnitude (Manley 1992). Assuming that a similar rule applies to 5- to 20-m-thick rhyolite bodies, and taking a magma viscosity of 10^6 Pa s, we calculate an effective lava flow viscosity of 10^8–10^9 Pa s. Using Jeffrey's equation for the flow of a viscous body on an inclined plane

$$v = \frac{\rho g h^2 \sin \alpha}{3\mu}$$

with magma density ρ=2500 kg m^{-3}, acceleration due to gravity g=9.8 m s^{-2}, thickness of viscous body h=20 m, slope angle α=30° and viscosity μ=10^8–10^9 Pa s, this gives a potential lava flow velocity of 10^{-3}–10^{-2} m s^{-1}.

Therefore, for the Bláhnúkur lava lobes, the potential lava flow velocity could have exceeded the ice melting rate by three or four orders of magnitude, so the ice would have constrained the lava.

Two independent observations from active volcanoes support this hypothesis. Vinogradov and Murav'ev (1988) observed that supraglacial meltwater runoff incised channels in the glacier downslope of the vent during an eruption in Kamchatka, which formed a mould for an ensuing lava flow. Basaltic lava from Okmok volcano, Alaska, was diverted when it flowed against a glacier (Byers et al. 1947). Slower-flowing rhyolite lavas are likely to be similarly diverted by ice walls. The implication is that the shape of lava bodies on Bláhnúkur may record the shape of cavities present at the glacier base during the eruption.

Evidence for the morphology of subglacial cavities

Lava lobes

The joint patterns, morphologies and distribution of rhyolite lava lobes suggest that conical ice cavities were melted into the base of the glacier during this phase of the eruption. From the sizes of the lava lobes, we infer that these cavities had roofs between 2 and 5 m high and were randomly distributed. There are three lines of evidence for magma–water interaction at lobe bases: perlitic alteration of obsidian; a gradational contact with breccia that contains blocky ash shards; and the presence of matrix vesicles in the breccia. From this it is inferred that the cavities contained at least some meltwater, although it is impossible to tell whether they were completely filled. Such a subglacial cavity system has not been described in the glaciological literature (e.g. Fountain and Walder 1998), and may reflect localised melting of the glacier base by convecting steam, possibly linked to lava lobe advance.

Columnar jointed lavas

Later in the eruption, it appears that much larger cavities had developed in the glacier base: over 20 m high and 20 m wide. These cavities had steeply inclined ice walls and may have contained little meltwater ("open" conditions; Hooke 1984), as the lack of evidence for magma–water interaction suggests. Subglacial cavities of a similar size are thought to have carried meltwater away from the site of the 1996 Gjálp eruption (Guðmundsson et al. 1997).

Position of the ice roof and eruptive mechanisms

Initially, the rate of outward growth of the edifice may have approximately matched the rate of melting of the surrounding ice, thus maintaining the ice roof close to the volcano. At this stage, lava lobes were emplaced in isolated ice cavities formed by localised melting of the glacier base (Fig. 10). Meanwhile, juvenile material was washed down the volcano flanks and redeposited by meltwater in subglacial channels (Fig. 10). We speculate that a hiatus in the eruption then followed, during which the ice roof receded significantly from the edifice (Fig. 11). Continued heat loss from newly erupted material via steam transport of heat to the ice roof would have allowed the subglacial cavities to enlarge without continuing to be filled with debris. As the ice retreated, portions of lava lobe-breccia A were locally destabilised and cascaded down the flanks, generating debris flow deposits (Fig. 10). After continued melting, a subsequent pulse of magma would have encountered larger cavities, the ice roof now up to 20 m above the edifice. Lavas then flowed down the slope within these cavities (Fig. 10).

Observations from a recent subglacial basalt eruption in Iceland support this model. Melting continued above the site of the 1998 Grímsvötn subglacial eruption for weeks after the eruption had stopped, as the hyaloclastite pile slowly cooled (M.T. Guðmundsson, pers. commun.).

Meltwater drainage and hazard implications

The presence of (a) juvenile-rich subglacial meltwater stream deposits, and (b) "dry" subglacial lava flows within the subglacial rhyolite sequence at Bláhnúkur, suggests that meltwater was able to drain away during the eruption. This is consistent with the model of Hoskuldsson and Sparks (1997), which predicted that positive volume changes accompanying subglacial rhyolite eruptions would expel meltwater from the vent area. A basaltic eruption underneath thin ice (<150 m) may also be well drained (Smellie and Skilling 1994).

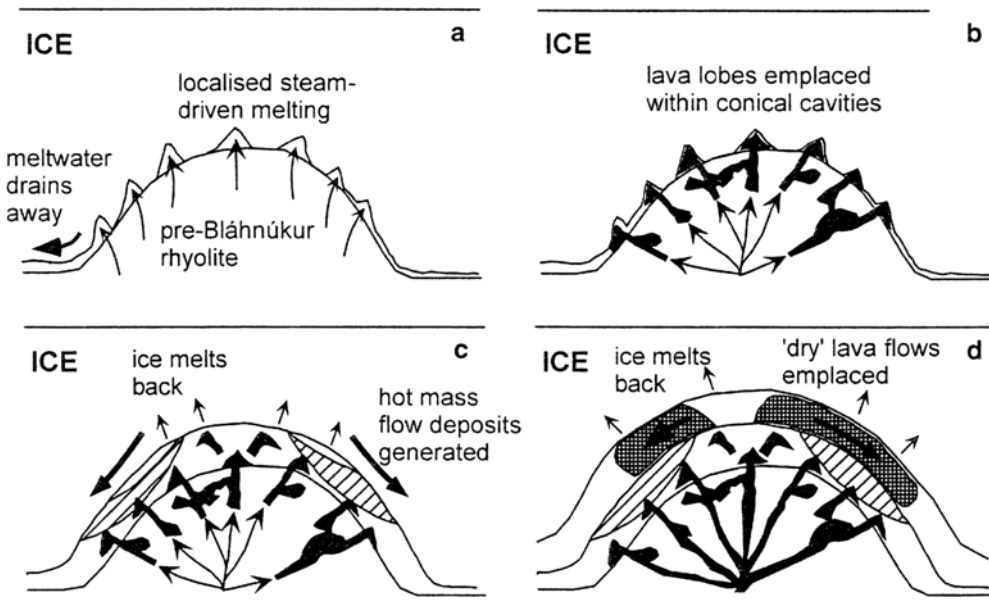

Fig. 10a–d The proposed sequence of events at Bláhnúkur. **a** Early eruptive products are reworked by meltwater in subglacial tunnels. Steam released from cooling lavas generates cavities in the glacier base. **b** Lava lobes and breccia A are emplaced within conical cavities in the ice. **c** Hot avalanche deposits are generated as the ice melts back from lava lobes and breccia. **d** "Dry" lava flows are emplaced within drained subglacial tunnels

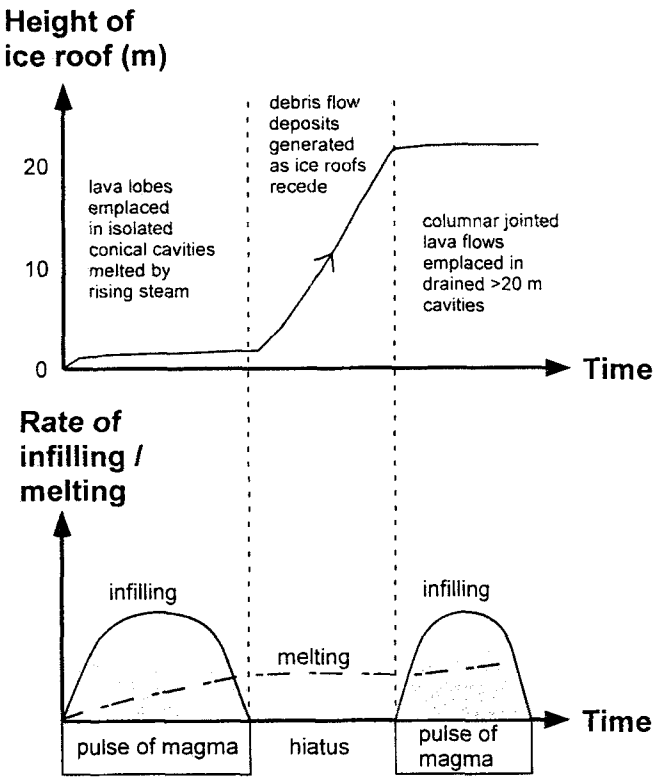

Fig. 11 Proposed variations in the ice roof height during the eruption (*top*) caused by a variable eruption rate (*bottom*)

However, Bláhnúkur was probably emplaced beneath a glacier >400 m thick, since the lithofacies suggest an entirely subglacial setting and the edifice is 350 m high; thus, we have strong evidence for basal leakage of meltwater under a thick glacier (Smellie 1999).

The lack of development of a subglacial lake at Bláhnúkur served to decrease the volcanic hazards in two ways: (a) by limiting the volume of standing water available for explosive magma–water interaction; and (b) by restricting the intensity of any resultant jökulhlaup.

Conclusion

Field observations of the effusive subglacial rhyolite succession at Bláhnúkur have revealed complex patterns of volcano-ice interaction. The ice roof was close to the growing edifice during the early stages of eruption, and lava lobes entered conical cavities melted in the glacier base. Only a minor volume of phreatomagmatic tephra was generated, largely at lobe bases. As the ice roof melted back, lava lobes and tephra were destabilised and cascaded down the volcano flanks. A variety of deposits indicates that avalanching occurred both during and after emplacement of the lava lobes. During the eruption, heat from the subglacial deposits enlarged existing subglacial cavities, forming moulds for subsequent lava flows that advanced and chilled against the ice walls. The presence or absence of water in the subglacial cavities appears to have controlled the eruption mechanisms. A complex feedback between the eruption rate, the ice melting rate and the eruption mechanisms resulted in the varied lithofacies architecture observed. Meltwater was able to drain away from the vent area during the eruption, reducing the volcanic hazards.

Acknowledgements We thank G. Finnsdottír, B. Sigmarsdottír, F. Eíriksson and D. Samuelsson of Ferðafelag Íslands for their help and hospitality during fieldwork. The willingness of K. Sæmundsson, G.O. Friðleifsson, H. Björnsson and M.T. Guðmundsson to share their expertise in Icelandic subglacial volcanism is much appreciated. Thanks to H. Pinkerton for useful discussions and B.H. Houghton for comments on the manuscript. The style and content of the article were enhanced by reviews by J.L. Smellie and I. Skilling. H. Tuffen was supported by an Open University research studentship. J. Gilbert's fieldwork was supported by a Lancaster University travel grant. D. McGarvie was supported by an Open University research grant.

References

Allen CC (1980) Icelandic subglacial volcanism: thermal and physical studies. J Geol 88:108–117

Byers FM, Hopkins DM, Wier KL, Fisher B (1947) Volcano investigations on Umnak Island 1946, Progress of investigations in 1946, part 3. US Geol Surv Alaskan Volcano Invest Rep 2:19–53

Cas RAF, Allen RL, Bull SW, Clifford BA, Wright JV (1990) Subaqueous, rhyolitic dome-top tuff cones: a model based on the Devonian Bunga beds, southeastern Australia and a modern analog. Bull Volcanol 52:159–174

DeGraff JM, Long PE, Aydin A (1989) Use of joint-growth directions and rock textures to infer thermal regimes during solidification of basaltic lava flows. J Volcanol Geotherm Res 38:309–324

Dugmore AG, Larsen G, Newton AJ (1995) 7 tephra isochrons in Scotland. Holocene 5:257–266

Fink JH (1983) Structure and emplacement of a rhyolitic obsidian flow: Little Glass Mountain, Medicine Lake Highland, northern California. Geol Soc Am Bull 94:362–380

Fountain AG, Walder JS (1998) Water flow through temperate glaciers. Rev Geophys 36:299–328

Furnes H, Friðleifsson IB, Atkins FB (1980) Subglacial volcanics: on the formation of acid hyaloclastites. J Volcanol Geotherm Res 8:95–110

Grönvold K (1972) Structural and petrochemical studies in the Kerlingarfjöll region, central Iceland. PhD thesis, Univ Oxford, 250 pp

Guðmundsson MT, Sigmundsson F, Björnsson H (1997) Ice-volcano interaction of the 1996 Gjálp subglacial eruption, Vatnajökull, Iceland. Nature 389:954–957

Hanson RE (1991) Quenching and disruption of andesitic to rhyolitic intrusions in a submarine island-arc sequence, northern Sierra Nevada, California. Geol Soc Am Bull 103:804–816

Heiken G, Wohletz K (1985) Volcanic ash. University of California Press, Berkeley

Higgins MD (1996) Magma dynamics beneath Kameni volcano, Thera, Greece, as revealed by crystal size and shape measurements. J Volcanol Geotherm Res 70:37–48

Hooke RL (1984) On the role of mechanical energy in maintaining subglacial water conduits at atmospheric pressure. J Glaciol 30:180–187

Hoskuldsson A, Sparks RSJ (1997) Thermodynamics and fluid dynamics of effusive subglacial eruptions. Bull Volcanol 59: 219–230

Hunns SR, McPhie J (1999) Pumiceous peperite in a submarine volcanic succession at Mount Chalmers, Queensland, Australia. J Volcanol Geotherm Res 88:239–254

Ivarsson G (1992) Geology and petrochemistry of the Torfajökull central volcano in central south Iceland, in association with the Icelandic hot spot and rift zones. PhD thesis, Univ Hawaii

Jones JG (1968) Intraglacial volcanoes of the Laugarvatn region, south-west Iceland, I. J Geol Soc Lond 124:197–211

Kokelaar BP (1982) Fluidization of wet sediments during the emplacement and cooling of various igneous bodies. J Geol Soc 139:21–33

Lacasse C, Sigurdsson H, Johannesson H, Paterne M, Carey S (1995) Source of Ash Zone 1 in the North Atlantic. Bull Volcanol 57:18–32

Larsen G, Guðmundsson MT, Björnsson H (1998) Eight centuries of periodic volcanism at the center of the Iceland hotspot revealed by glacier tephrostratigraphy. Geology 26:943–946

Lescinsky DT, Sisson TW (1998) Ridge-forming, ice-bounded lava flows at Mount Rainier, Washington. Geology 26:351–354

Lorenz V (1974) Vesiculated tuff and associated features. Sedimentology 21:273–291

Manley CR (1992) Extended cooling and viscous flow of large, hot rhyolite lavas: implications of numerical modelling results. J Volcanol Geotherm Res 53:27–46

McGarvie DW (1984) Torfajökull: a volcano dominated by magma mixing. Geology 12:685–688

McPhie J, Doyle M, Allen R (1993) Volcanic textures. A guide to the interpretation of textures in volcanic rocks. Tasmanian Government Printing Office, Tasmania, pp 1–196

Sæmundsson K (1970) Interglacial lava flows in the lowlands of southern Iceland and the problem of two-tiered columnar jointing. Jökull 20:62–77

Sæmundsson K (1972) Jarðfræðiglefsur um Torfajökulssvæðið. Natturufræðingurinn 42:81–99 (in Icelandic)

Sæmundsson K (1988) Jarðfræðiðattur um Torfajökulsöræfi. Arbok Ferðafelag Islands 164–180 (In Icelandic)

Scutter CR, Cas RAF, Moore CL, Derita D (1998) Facies architecture and origin of a submarine rhyolitic lava flow-dome complex, Ponza, Italy. J Geophys Res 103:27551–27566

Skilling IP (1994) Evolution of an englacial volcano: Brown Bluff, Antarctica. Bull Volcanol 56:573–591

Smellie JL (1999) Subglacial eruptions. In: Sigurdsson H (ed) Encyclopaedia of volcanoes. Academic Press, San Diego, pp 403–418

Smellie JL, Hole MJ (1997) Products and processes in Pliocene–Recent, subaqueous to emergent volcanism in the Antarctic Peninsula: examples of englacial Surtseyan volcano construction. Bull Volcanol 58:628–646

Smellie JL, Skilling IP (1994) Products of subglacial volcanic eruptions under different ice thicknesses: two examples from Antarctica. Sediment Geol 91:115–129

Smellie JL, Hole MJ, Nell PAR (1993) Late Miocene valley-confined subglacial volcanism in Northern Alexander Island, Antarctic Peninsula. Bull Volcanol 55:273–288

Vinogradov VN, Murav'ev YD (1988) Lava–ice interaction during the 1983 Klyuchevskoi eruption. Volcanol Seismol 7:39–61

Werner R, Schmincke H-U (1999) Englacial vs lacustrine origin of volcanic table mountains: evidence from Iceland. Bull Volcanol 60:335–354

Werner R, Schmincke HU, Sigvaldason G (1996) A new model for the evolution of table mountains: volcanological and petrological evidence from Herðubreið and Herðubreiðartogl volcanoes (Iceland). Geol Rundsch 85:390–397

White JDL, Busby-Spera CJ (1987) Deep marine arc apron deposits and syndepositional magmatism in the Alisitos group at Punta Cono, Baja California, Mexico. Sedimentology 34:911–927

Yamagishi H, Dimroth E (1985) A comparison of Miocene and Archean rhyolite hyaloclastites: evidence for a hot and fluid rhyolite lava. J Volcanol Geotherm Res 23:337–355

Zielinski GA, Mayewski PA, Meeker LD, Grönvold K, Germani MS, Whitlow S, Twickler MS, Taylor K (1997) Volcanic aerosol records and tephrochronology of the Summit, Greenland, ice cores. J Geophys Res 102:26625–26640